



ELSEVIER

Available online at

ScienceDirect
www.sciencedirect.com

Elsevier Masson France

EM|consulte
www.em-consulte.com/en



CLINICAL RESEARCH

Clinical and prognostic implications of phenomapping in patients with heart failure receiving cardiac resynchronization therapy[☆]

Implications cliniques et pronostiques du phéno-mapping chez les patients insuffisants cardiaques implantés d'une thérapie de resynchronisation cardiaque

Clémence Riolet^a, Aymeric Menet^a,
Stéphane Verdun^b, Alexandre Altes^{a,1},
Ludovic Appert^a, Yves Guyomar^a, François Delelis^a,
Pierre Vladimir Ennezat^c, Raphaëlle A. Guerbaai^d,
Pierre Graux^a, Christophe Tribouilloy^{e,f},
Sylvestre Marechaux^{a,f,2,3,*}

^a Cardiology Department, Lille Catholic Hospitals, Lille Catholic University, 59160 Lomme, France

^b Biostatistics Department—Delegations for Clinical Research and Innovation, Lille Catholic Hospitals, Lille Catholic University, 59160 Lille, France

^c Henri Mondor University Hospital, 94010, Créteil, France

^d Department of Public Health (DPH), Faculty of Medicine, Basel University, 4056 Basel, Switzerland

Abbreviations: BNP, brain natriuretic peptide; CRT, cardiac resynchronization therapy; HF, heart failure; HFREF, heart failure with reduced ejection fraction; ICD, implantable cardioverter defibrillator; LBBB, left bundle branch block; LV, left ventricle/ventricular; LVEF, left ventricular ejection fraction; LVESV, left ventricular end-systolic volume; PCA, principal component analysis; RV, right ventricular.

[☆] Tweet: Machine learning to predict outcome after CRT? A new study demonstrating the prognostic implications of phenomapping in patients with heart failure receiving cardiac resynchronization therapy.

* Corresponding author at: Cardiology Department, Hôpital Saint Philibert, 115 rue du Grand But, 59462 Lomme Cedex, France.

E-mail address: sylvestre.marechaux@gmail.com (S. Marechaux).

¹ Twitter address: @MarechauxSyl.

² Twitter address: @alexandre.altes.

³ Twitter address: @ghicl.

<https://doi.org/10.1016/j.acvd.2020.07.004>

1875-2136/© 2020 Elsevier Masson SAS. All rights reserved.

Please cite this article in press as: Riolet C, et al. Clinical and prognostic implications of phenomapping in patients with heart failure receiving cardiac resynchronization therapy. Arch Cardiovasc Dis (2020), <https://doi.org/10.1016/j.acvd.2020.07.004>

^e Amiens University Hospital, 80080 Amiens, France

^f Laboratory MP3CV–EA 7517, University Centre for Health Research, Picardy University, 80000 Amiens, France

Received 27 May 2020; received in revised form 23 June 2020; accepted 1st July 2020

KEYWORDS

Cardiac
resynchronization
therapy;
Heart failure;
Outcome;
Echocardiography;
Phenomapping

Summary

Background. – Despite having an indication for cardiac resynchronization therapy according to current guidelines, patients with heart failure with reduced ejection fraction who receive cardiac resynchronization therapy do not consistently derive benefit from it.

Aim. – To determine whether unsupervised clustering analysis (phenomapping) can identify distinct phenogroups of patients with differential outcomes among cardiac resynchronization therapy recipients from routine clinical practice.

Methods. – We used unsupervised hierarchical cluster analysis of phenotypic data after data reduction (55 clinical, biological and echocardiographic variables) to define new phenogroups among 328 patients with heart failure with reduced ejection fraction from routine clinical practice enrolled before cardiac resynchronization therapy. Clinical outcomes and cardiac resynchronization therapy response rate were studied according to phenogroups.

Results. – Although all patients met the recommended criteria for cardiac resynchronization therapy implantation, phenomapping analysis classified study participants into four phenogroups that differed distinctively in clinical, biological, electrocardiographic and echocardiographic characteristics and outcomes. Patients from phenogroups 1 and 2 had the most improved outcome in terms of mortality, associated with cardiac resynchronization therapy response rates of 81% and 78%, respectively. In contrast, patients from phenogroups 3 and 4 had cardiac resynchronization therapy response rates of 39% and 59%, respectively, and the worst outcome, with a considerably increased risk of mortality compared with patients from phenogroup 1 (hazard ratio 3.23, 95% confidence interval 1.9–5.5 and hazard ratio 2.49, 95% confidence interval 1.38–4.50, respectively).

Conclusions. – Among patients with heart failure with reduced ejection fraction with an indication for cardiac resynchronization therapy from routine clinical practice, phenomapping identifies subgroups of patients with differential clinical, biological and echocardiographic features strongly linked to divergent outcomes and responses to cardiac resynchronization therapy. This approach may help to identify patients who will derive most benefit from cardiac resynchronization therapy in “individualized” clinical practice.

© 2020 Elsevier Masson SAS. All rights reserved.

MOTS CLÉS

Thérapie de
resynchronisation
cardiaque ;
Insuffisance
cardiaque ;
Pronostic ;
Speckle tracking ;
Échocardiographie ;
Phénomapping

Résumé

Contexte. – Bien qu'ils aient une indication de thérapie de resynchronisation cardiaque (TRC) selon les recommandations actuelles, les patients souffrant d'insuffisance cardiaque à fraction d'éjection altérée (IC-FEA) recevant une TRC ne tirent pas systématiquement bénéfice de celle-ci. Nous avons émis l'hypothèse que parmi les receveurs d'une TRC en pratique clinique courante, une analyse en clusters non supervisée (phénomapping) pourrait identifier des phénogroupes distincts de patients avec des pronostics différents.

Méthodes. – Une analyse hiérarchique en clusters non supervisée des données phénotypiques après réduction des données (55 variables cliniques, biologiques et échocardiographiques) a été réalisée pour définir de nouveaux phénogroupes parmi 328 patients souffrant d'IC-FEA implantés d'une TRC selon les indications classiques. Les résultats cliniques et le taux de réponse à la TRC ont été étudiés en fonction des phénogroupes.

Résultats. – Tous les patients remplissaient les critères recommandés pour l'implantation d'une TRC; cependant l'analyse phénotypique a classé les participants à l'étude en 4 groupes, différant distinctement en termes de caractéristiques cliniques, biologiques, électrocardiographiques et échocardiographiques. Les patients des groupes 1 et 2 avaient un meilleur pronostic en termes de mortalité, avec un taux de réponse à la TRC de 81 % et 78 % respectivement. En revanche, les patients des groupes 3 et 4 avaient un taux de réponse à la TRC de 39 % et 59 % respectivement, et un moins bon pronostic avec un risque de mortalité

considérablement accru par rapport aux patients du groupe 1 (HR 3,23, IC95 % [1,9–5,5] et 2,49, IC95 % [1,38–4,50] respectivement).

Conclusions. – Parmi les patients souffrant d'IC-FEA avec une indication de TRC en pratique clinique de routine, le phenomapping a identifié des sous-groupes de patients présentant des caractéristiques cliniques, biologiques et échocardiographiques différentes fortement liées au pronostic et à la réponse à la TRC. Cette approche pourrait aider à identifier les patients qui tirent le plus d'avantages de la TRC, pour une pratique clinique « individualisée ».

© 2020 Elsevier Masson SAS. Tous droits réservés.

Background

Cardiac resynchronization therapy (CRT) is currently recommended to improve symptoms, left ventricular (LV) function and prognosis in patients with moderate-to-severe heart failure with reduced ejection fraction (HFrEF) and prolonged QRS duration [1]. The current recommended guidelines for CRT are derived from the findings of randomized controlled therapeutic trials, which enabled a dramatic improvement in the therapeutic management of patients with HFrEF and prolonged QRS duration. However, an overall benefit does not exclude that some patients may be harmed by or will not respond to the therapeutic agent under study. Indeed, despite meeting currently recommended clinical and electrocardiographic criteria for CRT implantation, 20–40% of patients with HFrEF and prolonged QRS duration fail to respond to CRT and have a poor outcome, despite continuous improvement in CRT devices and heart failure (HF) management [2]. An individualized approach is clearly needed to identify and treat patients who are more likely to be able to benefit from CRT. Therefore, understanding the phenotypic heterogeneity of patients with HFrEF receiving CRT may help to identify similar individuals who may respond in a more homogeneous and predictable way to CRT.

Numerous clinical, electrocardiographic, biological and echocardiographic data have been linked to outcome and response to CRT [3–13]. However, it remains unclear how these variables are linked, and whether some of the characteristics are shared by patients with the same phenotype. Classical statistical adjustment in multivariable modelling allows several variables of potential importance to be taken into account, but does not provide information about the phenotype of patients. In contrast, unsupervised machine learning methods (i.e. phenomapping) can be used to analyse complex features associated with various therapeutic responses. This approach may be useful to resolve heterogeneity in patients with similar syndromes, but heterogeneous characteristics and outcome, such as patients with HF syndromes receiving CRT. Hence, in the present report, we used an unsupervised phenomapping approach in patients with HFrEF receiving CRT in routine daily practice.

The hypotheses behind the present study were that: (1) phenomapping might help to identify homogeneous groups of patients among CRT recipients, in terms of clinical, electrocardiographic, biological and echocardiographic profiles; and (2) the identified patient phenogroups would have differential outcomes and response rates following CRT.

Methods

The authors are solely responsible for the design and conduct of this study, all study analyses, the drafting and editing of the paper and its final contents.

Study population

The present population consisted of 328 ambulatory patients with HF referred to Hôpital Saint Philibert, Lomme, France, for CRT device implantation between 2010 and 2017, according to current clinical practice guidelines [6]. Left bundle branch block (LBBB) morphology was defined according to American College of Cardiology/American Heart Association guidelines [14]. Exclusion criteria have been detailed elsewhere [11]. Patients received maximally tolerated doses of HF medications. The study was approved by the Lille Catholic University ethics committee for non-interventional research. Informed consent was obtained from all patients at the time of enrolment. The trial was registered on ClinicalTrials.gov (Identifier: NCT02986633).

CRT device implantation

Boston Scientific (Natick, MA, USA), Medtronic (Minneapolis, MN, USA), St. Jude Medical (St Paul, MN, USA), Sorin (Milan, Italy), and Biotronik (Berlin, Germany) CRT devices were implanted by electrophysiologists targeting a basal lateral, anterolateral or posterolateral coronary sinus vein for LV lead positioning. Interventricular timing was set at zero. A short-sensed atrioventricular delay (between 80 and 100 ms) and a paced delay (130 ms) were programmed to promote biventricular pacing. For patients with uncontrolled atrial fibrillation, radiofrequency ablation of the atrioventricular node was performed if sufficient bradycardia was not obtained despite optimal medical treatment, in order to obtain a high percentage of biventricular pacing.

Phenotypic data

Epidemiological, clinical and biological data

Epidemiological, clinical and biological characteristics collected in the present study are detailed in Table 1. Blood was sampled in the supine position for serum creatinine and plasma brain natriuretic peptide (BNP) concentrations the day before CRT device implantation. The aetiology of LV dysfunction was deemed to be ischaemic in case of a history

Table 1 Baseline characteristics of the study population ($n = 328$).

Epidemiological data	
Age (years)	72 ± 11
Male sex	209 (64)
Clinical data	
BMI (kg/m ²)	26 (23; 30)
SBP (mmHg)	120 (110; 135)
HR (beat/min)	70 (62; 80)
NYHA III/IV	167 (51)
Diabetes mellitus	98 (30)
Hypertension	167 (51)
Dyslipidaemia	152 (47)
History of AF	107 (33)
AF during echocardiography	58 (20)
CAD	122 (37)
COPD	53 (16)
Beta-blocker	290 (89)
ACE inhibitor/ARB	285 (88)
Aldosterone antagonist	94 (29)
Diuretic	260 (80)
ICD	262 (80)
Upgrading to CRT	77 (24)
9-month percentage of BVP (%)	97 ± 10
Electrocardiogram data	
Baseline QRS duration (ms)	160 (150; 180)
QRS morphology	
LBBB	236 (72)
RBBB	7 (2)
Non-specific IVCD	38 (12)
RV pacing	47 (14)
BVP QRS duration (ms)	140 (120; 150)
Effective BVP	262 (83)
Biological data	
Creatinine (mg/L)	12 (9; 15)
BNP (pg/mL)	433 (190; 941)
Lead position on chest X-ray	
Non-apical LV lead position	248 (83)
Lateral versus non-lateral LV lead position	
Lateral (lateral)	137 (46)
Posterior (lateral)	146 (49)
Anterior (non-lateral)	3 (1)
Anterolateral (non-lateral)	14 (5)
RV lead position	
Apical RV lead position	33 (10)
Free wall RV lead position	41 (13)
High septum RV lead position	5 (2)
Mid septum RV lead position	224 (72)
RVOT RV lead position	10 (3)
Echocardiographic data	
LVEDV (mL)	231 (187; 284)
LVESV (mL)	168 (136; 208)
LVEF (%)	27 ± 6
GLS (%)	-7.5 (-9.5; -5.8)
LV mass index (g/m ²)	150 (127; 176)
Cardiac output index (L/m ²)	2.2 (1.8; 2.8)
LA volume index (mL/m ²)	37 (28; 46)
E-wave deceleration time (ms)	155 (127; 223)
E-wave velocity (m/s)	0.8 (0.6; 1)

Table 1 (Continued)

E/A ratio	0.9 (0.6; 1.8)
E/E' ratio	13 (10; 17)
Mitral ERO (mm ²)	0 (0; 8)
No. of LV scarred segments	1 ± 2
RV diameter (mm)	31 ± 7
RA volume index (mL/m ²)	44 (30; 68)
TR peak velocity (m/s)	2.8 ± 0.6
Estimated RA pressure (mmHg)	5 (3; 8)
TAPSE (mm)	20 ± 8
Grade 3 or 4 TR	34 (11)
Interventricular dyssynchrony:	46 (26; 64)
IVMD (ms)	
Atrioventricular dyssynchrony:	40 ± 9
ratio of the LV filling and RR interval (%)	
Septal flash	189 (84)
Apical rocking	156 (66)
Longitudinal LBBB classical pattern	276 (89)
Radial LBBB classical pattern	102 (54)
Septal deformation pattern 1 or 2	196 (59)

Quantitative data are expressed as mean ± standard deviation or median (25th; 75th percentile); qualitative data are expressed as absolute number (%). ACE: angiotensin-converting enzyme; AF: atrial fibrillation; ARB: angiotensin receptor blocker; BMI: body mass index; BNP: brain natriuretic peptide; BVP: biventricular pacing; CAD: coronary artery disease; COPD: chronic obstructive pulmonary disease; CRT: cardiac resynchronization therapy; ERO: effective regurgitant orifice; GLS: global longitudinal strain; HR: heart rate; ICD: implantable cardioverter defibrillator; IVCD: intraventricular conduction delay; IVMD: interventricular mechanical delay; LA: left atrial; LBBB: left bundle branch block; LV: left ventricular; LVEDV: left ventricular end-diastolic volume; LVEF: left ventricular ejection fraction; LVESV: left ventricular end-systolic volume; NYHA: New York Heart Association; RA: right atrial; RBBB: right bundle branch block; RV: right ventricular; RVOT: right ventricular outflow tract; SBP: systolic blood pressure; TAPSE: tricuspid annular plane systolic excursion; TR: tricuspid regurgitation.

of myocardial infarction or significant coronary artery disease on coronary angiography (> 50% stenosis of an epicardial vessel).

Electrocardiogram and LV lead position

A twelve-lead electrocardiogram was performed the day before and the day after CRT implantation. All measurements were performed off-line with millimeter paper by a single investigator blinded to clinical and outcome data. QRS duration before and after CRT implantation was measured in the electrocardiogram derivation showing the wider QRS, as previously reported [4,10]. Relative QRS narrowing (Δ QRS%) was the subtraction of postoperative QRS duration from the preoperative QRS duration divided by the preoperative QRS duration. Biventricular paced QRS morphology was defined as positive when there was a prominent R wave in lead V1 (R/S ratio ≥ 1 in lead V1) and/or a prominent S wave in lead I (R/S ratio ≤ 1 in lead I) on the postprocedural electrocardiogram. Location of the LV lead was determined using

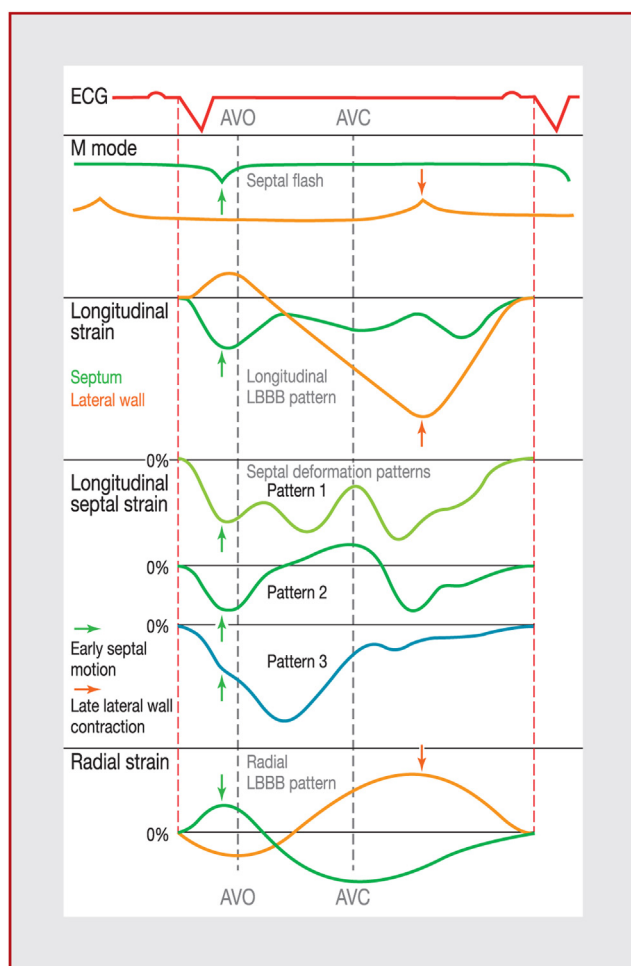


Figure 1. Echocardiographic assessment of electromechanical dyssynchrony. AVC: aortic valve closing; AVO: aortic valve opening; ECG: electrocardiogram; LBBB: left bundle branch block.

postoperative anteroposterior and lateral chest radiography [15].

Echocardiography

Echocardiography was performed the day before CRT device implantation and at 9-month follow-up by one investigator blinded to the clinical status of the patient, using the Vivid E9 or E95 ultrasound system (GE Healthcare, Velizy, France).

Standard echocardiographic measurements were performed according to the European Association of Cardiovascular Imaging guidelines, and as previously reported [11,16]. Longitudinal two-dimensional speckle-tracking strain curves were analysed offline using a dedicated workstation, as previously reported (EchoPAC PC, release BT11; GE Vingmed Ultrasound AS; GE Healthcare, Velizy, France) [11].

Various echocardiographic electromechanical dyssynchrony data were gathered. Septal flash was defined as an early septal thickening/thinning within the isovolumic contraction period, as detected visually from the grayscale short-axis and four-chamber views, and from the parasternal long-axis, short-axis and four-chamber views obtained by M-mode (Fig. 1) [17]. Apical rocking, identified in apical four-chamber view, is characterized by a short septal

motion of the apex as a result of the early contraction of the septum in systole, and a subsequent long motion to the lateral side during ejection, as a result of the late lateral contraction caused by the LBBB. This rocking movement results in a clockwise motion of the LV apical myocardium perpendicular to the LV long axis [9]. A classical LBBB pattern of contraction was searched for, using both radial and longitudinal strain waveforms (Fig. 1), and was defined as an early contraction of the septal or anteroseptal wall and early stretching in the opposing wall [18,19]. Septal deformation patterns were classified on the basis of the septal shortening and stretching sequence [20,21]. Three patterns were characterized (Fig. 1): double-peaked systolic shortening (pattern 1); early pre-ejection shortening followed by prominent systolic stretch (pattern 2); and pseudonormal shortening with a late systolic shortening peak, no or minimal pre-ejection septal lengthening and less pronounced end-systolic stretch (pattern 3). Unlike pattern 3, patterns 1 and 2 have previously been associated with a high probability of CRT response and a favourable outcome [11,21]. Interventricular dyssynchrony was assessed using interventricular mechanical delay, which is the difference between LV and right ventricular (RV) pre-ejection delays. Atrioventricular dyssynchrony was assessed by calculating the ratio of the LV filling time and RR interval.

Outcomes

During follow-up, patients were monitored by their own private physicians. Events were recorded by clinical interviews and/or by telephone calls to physicians, patients and (if necessary) next of kin. Autopsy records and death certificates were consulted for attribution of causes of death. The primary endpoint of the study was overall mortality, and secondary endpoints were cardiovascular mortality and hospitalization for HF. Cardiovascular mortality was considered if death was related to HF, myocardial infarction, arrhythmia or sudden death.

Change in LV end-systolic volume (Δ LVESV) was defined as the extent of reduction in LVESV between baseline and 9-month follow-up relative to baseline LVESV. Response to CRT was defined as Δ LVESV \geq 15%. Super-response to CRT was defined as an absolute LV ejection fraction (LVEF) \geq 45% at 9-month follow-up.

Statistical analysis

Detailed statistical analysis information can be found in the Appendix B.

Variable reduction

Clustering of variables was performed with the ClustOfVar package in R [22]. This package allows groups of variables to be found, and each group to be summarized by a new variable. The detailed method is depicted in the Appendix B. Briefly, the hierarchical clustering method was used here among a total of 55 phenotypic variables (Table 1), without outcome data, as previously described by Chavent et al. [22]. The numbers of clusters of variables were determined visually using a dendrogram. For each cluster, a principal component analysis (PCA) was performed, and a single vari-

able was kept, corresponding to the first component of the PCA, a linear combination of all variables defining the cluster.

Phenomapping of patients

Agglomerative hierarchical clustering was used on the six phenotypic variables obtained by variable reduction to obtain phenogroups of patients, with visual determination of the optimal number of phenogroups on a dendrogram. The `hclust` function in R was used for hierarchical clustering. The stability of the phenogroups was internally validated using a bootstrap approach with 100 iterations, and quantified using the Rand indices [23].

Analysis

Quantitative data are presented as means \pm standard deviations or medians (25th; 75th percentiles) in case of skewness and/or deviation of normality assumption. Qualitative data are presented as absolute numbers and percentages. The duration of follow-up was computed for each endpoint using the reverse Kaplan-Meier method. Survival curves were obtained using the Kaplan-Meier method.

Univariate Cox models were used to identify the relationship between phenotypic groups of patients and occurrence of events during follow-up. The proportional hazards assumption was confirmed using tests and graphs on the basis of the Schoenfeld residuals. For continuous variables, the assumption of linearity was assessed by plotting residuals against independent variables. The proportions of CRT responders and super-responders were calculated for each cluster of patients; the 95% confidence interval (CI) of this proportion was calculated using a bootstrap approach.

For all tests, a two-tailed P value < 0.05 was considered statistically significant. Statistical analysis was performed with R 3.4.2 (Youngstown, OH, USA) by the Biostatistics Department of the Delegation for Clinical Research and Innovation of Lille Catholic University Hospitals.

Results

Three hundred and twenty-eight patients were included in the present study. The mean age was 72 ± 11 years and 64% of patients were male. The characteristics of the study population are detailed in Table 1. The mean QRS width was 163 ± 25 ms, and 72% of patients had a LBBB configuration on the electrocardiogram. Eighty per cent of the study population received an implantable cardioverter defibrillator (ICD). The right ventricle was paced in 14% of patients.

Classification of phenotypic data

As shown in Fig. 2A and Table 2, six clusters of variables were obtained. Grossly, each variable cluster can be associated with distinct characteristics: clusters 1 and 2 correspond to epidemiological and/or clinical data, cluster 3 corresponds to LV geometry and function, cluster 4 corresponds to echocardiographic variables of dyssynchrony, cluster 5 corresponds to clinical, biological and echocardiographic data of HF severity and cluster 6 corresponds to electrocardiogram indices of electrical dyssynchrony.

Classification of patients

As shown in Fig. 2B and Table 3, four phenogroups of patients were obtained: 101 patients in phenogroup 1, 80 patients in phenogroup 2, 84 patients in phenogroup 3 and 63 patients in phenogroup 4. The mean bootstrap Rand index was 0.78 (95% CI 0.71–0.90), indicating a fair stability of the partition in four groups. In addition, removal of postimplant variables from Table 1 did not substantially alter variable clustering and patient phenogroups. The Rand index obtained by comparing phenogroups with and without postimplant variables was fair at 0.78, thereby indicating similar results. As expected, the four phenogroups of patients differed markedly. Characteristic features of each phenogroup are indicated in Table 3.

Patients from phenogroup 1 were more frequently women, with a high proportion of LBBB on the electrocardiogram and a very high proportion of echocardiographic electromechanical dyssynchrony, and more frequently experienced QRS narrowing following CRT. These patients had features of less advanced stages of the disease, including better LVEF and global longitudinal strain, preserved RV function, smaller cardiac cavities, lower plasma BNP concentrations and lower left- and right-sided Doppler-estimated intracardiac pressures.

Patients from phenogroup 2 were more frequently male and had lower systolic blood pressure, but similar electrical and electromechanical dyssynchrony compared with patients from phenogroup 1. Despite having mildly elevated plasma BNP concentrations and left- and right-sided Doppler-estimated intracardiac pressures, phenogroup 2 patients had the most dilated left ventricles (LVs), with the most depressed LV function, as indicated by LVEF and global longitudinal strain. In contrast, RV size and function were normal in phenogroup 2.

Patients from phenogroup 3 were more frequently male and in atrial fibrillation, and more frequently had reduced renal function compared with patients from phenogroups 1 and 2. Fewer patients had prolonged QRS and LBBB on the electrocardiogram. The frequency of echocardiographic electromechanical dyssynchrony was low in this patient phenogroup, and postoperative QRS narrowing was encountered less frequently. Ischaemic aetiology was more frequent in this phenogroup of patients, with a higher proportion of myocardial scar, severely enlarged LVs and severely depressed LV systolic function. RV function was also more frequently depressed in this subgroup of patients, and the right atrium was severely dilated. These patients more frequently experienced severe HF symptoms, as indicated by the higher frequency of New York Heart Association functional class III–IV, relatively high plasma BNP concentrations and elevated left- and right-sided Doppler-estimated intracardiac pressures.

Patients from phenogroup 4 were older, and therefore received ICD-CRT less frequently. RV pacing was frequently encountered. Atrial fibrillation and decreased renal function were highly prevalent, and these patients less frequently received renin-angiotensin-aldosterone system blockers. Echocardiographic indices of electromechanical dyssynchrony were found frequently, although septal deformation pattern 1 or 2 was found in only 57% of patients.

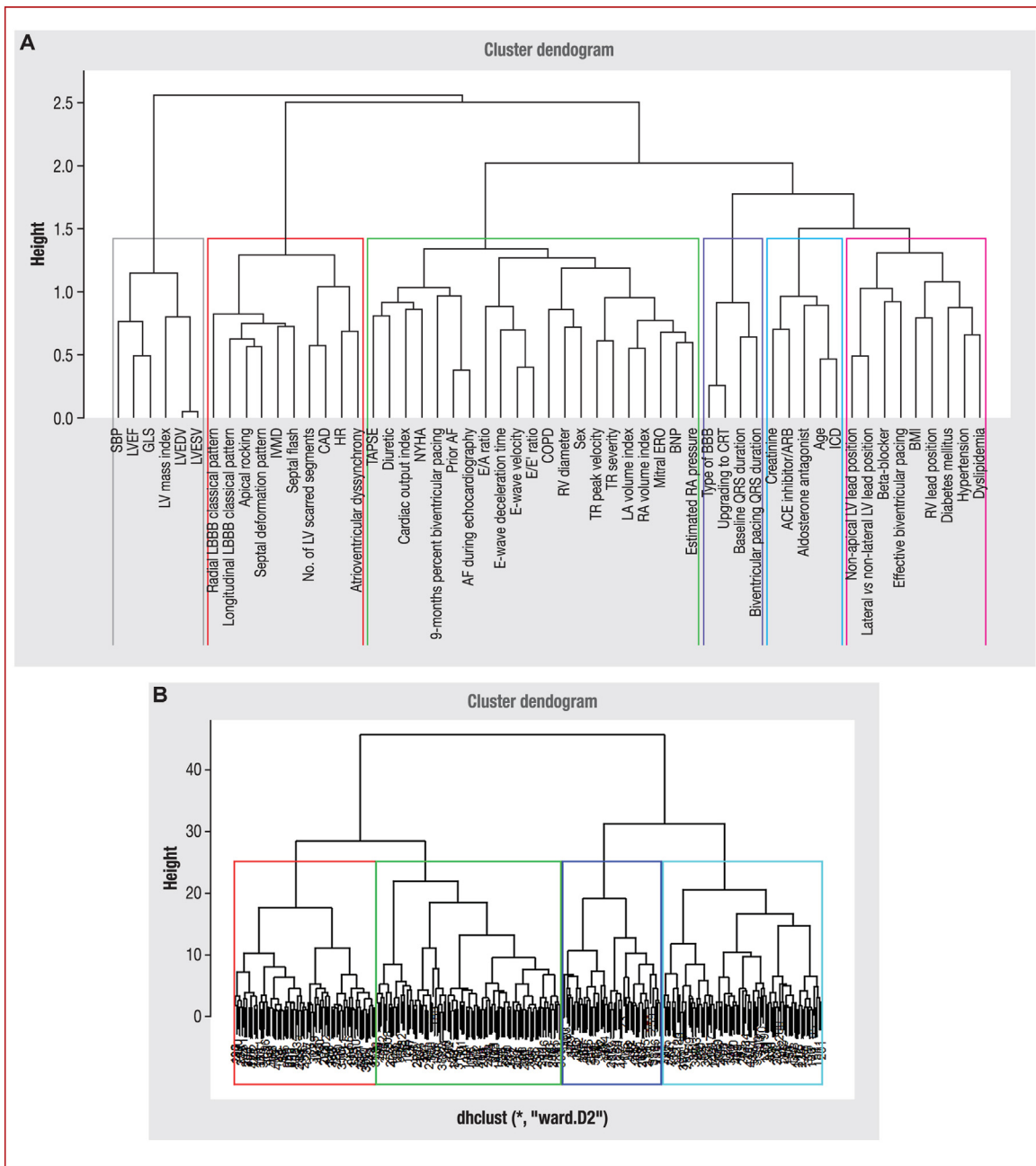


Figure 2. A, cluster dendrogram of phenotypic variables; B, cluster dendrogram of patients. ACE: angiotensin-converting enzyme; AF: atrial fibrillation; ARB: angiotensin receptor blocker; BBB: bundle branch block; BMI: body mass index; BNP: brain natriuretic peptide; CAD: coronary artery disease; COPD: chronic obstructive pulmonary disease; CRT: cardiac resynchronization therapy; ERO: effective regurgitant orifice; GLS: global longitudinal strain; HR: heart rate; ICD: implantable cardioverter defibrillator; IVMD: interventricular mechanical delay; LA: left atrial; LBBB: left bundle branch block; LV: left ventricular; LVEDV: left ventricular end-diastolic volume; LVEF: left ventricular ejection fraction; LVESV: left ventricular end-systolic volume; NYHA: New York Heart Association; RA: right atrial; RV: right ventricular; SBP: systolic blood pressure; TAPSE: tricuspid annular plane systolic excursion; TR: tricuspid regurgitation.

Interestingly, compared with patients from phenogroups 2 and 3, patients from phenogroup 4 exhibited features of a restrictive cardiac physiology, including relatively small LVs, severely enlarged left and right atria and more severe mitral and tricuspid regurgitation. Similarly, these patients had more severe HF symptoms (75% in New York Heart Association functional class III–IV), the highest plasma BNP concentrations and heightened left- and right-sided Doppler-estimated intracardiac pressures.

Impact of patient phenogroup on outcome and response to CRT

No patient was lost to follow-up. The median duration of follow-up was 51 (36; 72) months. During follow-up, 104 patients died (59 from cardiovascular causes), and 62 were hospitalized for HF. As shown in Fig. 3, phenogroup was associated with overall mortality (Fig. 3A) and cardiovascular mortality (Fig. 3B) (both $P < 0.0001$). Survival free from

Table 2 Clusters of phenotypic variables.

Cluster 1	Cluster 2	Cluster 3	Cluster 4	Cluster 5	Cluster 6
Age COPD	BMI Diabetes mellitus	Male SBP	HR CAD	NYHA History of AF	Upgrading to CRT Baseline QRS duration Type of BBB
ACE inhibitor/ARB	Hypertension	9-month % of BVP	Number of LV scarred segments	AF during TTE	BVP QRS duration
Aldosterone antagonist ICD	Dyslipidaemia Beta-blocker	LVEF LVEDV	IVMD Ratio of LV filling and RR interval	Diuretic BNP	
Creatinine	Effective BVP	LVESV	Septal flash	Cardiac output index LA volume index	
	Non-apical versus apical LV lead position	LV mass index	Apical rocking	E-wave deceleration time	
	Lateral versus non-lateral LV lead position RV lead position	GLS	Longitudinal LBBB classical pattern	E-wave velocity	
			Radial LBBB classical pattern	E/A ratio	
			Septal deformation pattern	E/E' ratio Mitral ERO RV diameter RA volume index TR peak velocity Estimated RA pressure TAPSE TR severity	

ACE: angiotensin-converting enzyme; AF: atrial fibrillation; ARB: angiotensin receptor blocker; BBB: bundle branch block; BMI: body mass index; BNP: brain natriuretic peptide; BVP: biventricular pacing; CAD: coronary artery disease; COPD: chronic obstructive pulmonary disease; CRT: cardiac resynchronization therapy; ERO: effective regurgitant orifice; GLS: global longitudinal strain; HR: heart rate; ICD: implantable cardioverter defibrillator; IVMD: interventricular mechanical delay; LA: left atrial; LBBB: left bundle branch block; LV: left ventricular; LVEDV: left ventricular end-diastolic volume; LVEF: left ventricular ejection fraction; LVESV: left ventricular end-systolic volume; NYHA: New York Heart Association; RA: right atrial; RBBB: right bundle branch block; RV: right ventricular; SBP: systolic blood pressure; TAPSE: tricuspid annular plane systolic excursion; TR: tricuspid regurgitation.

overall and cardiovascular mortality was similar in patients from phenogroup 1 and phenogroup 2 ($P=0.78$ and $P=0.47$, respectively), as well as in phenogroups 3 and 4 ($P=0.34$ and $P=0.30$, respectively). Similarly, time to first HF hospitalization (Fig. 3C) was statistically different according to each phenogroup, with similar HF hospitalization rates in phenogroups 1 and 2 ($P=0.30$), and a non-significant lower risk of HF hospitalization in patients from phenogroup 4 compared with those from phenogroup 3 ($P=0.063$).

Patients from phenogroup 3 and phenogroup 4 experienced an increased risk of mortality compared with patients from phenogroup 1 (hazard ratio 3.23, 95% CI 1.9–5.5 and hazard ratio 2.49, 95% CI 1.38–4.50, respectively) (Fig. 4A). The hazard ratios for cardiovascular mortality and HF hospitalization are depicted in Fig. 4B and Fig. 4C.

As depicted in Table 3, patients from phenogroups 1 and 2 experienced CRT response very frequently (81% and 78%, respectively), whereas the CRT response rate was

lower in patients from phenogroups 3 and 4 (39% and 59%, respectively). Most patients from phenogroup 1 (65%) experienced CRT super-response, whereas the proportion of CRT super-responders was significantly lower in the other patient phenogroups (Table 3).

The findings of the present study are summarized in the Central illustration (Fig. 5).

Discussion

In this prospective cohort of 328 patients with HFReF receiving CRT in routine clinical practice, unsupervised phenomapping analysis allowed the identification of phenogroups of patients with similar demographic, clinical, echocardiographic and biological features. Importantly, these phenogroups of patients had different clinical outcomes and CRT response rates, despite having classical

Table 3 Clusters of patients obtained after classification of variables.

	Phenogroup 1 (n = 101)	Phenogroup 2 (n = 80)	Phenogroup 3 (n = 84)	Phenogroup 4 (n = 63)	Overall P
Epidemiological data					
Age (years)	72 ± 10	66 ± 13	74 ± 10	78 ± 7 ^a	< 0.0001
Male sex	50 (50)	57 (71) ^a	66 (79) ^a	36 (57)	0.00017
Clinical data					
BMI	28 (25; 31)	25 (22; 29)	27 (24; 31)	26 (23; 29)	0.021
SBP	130 (119; 145)	120 (100; 130)	120 (110; 133)	119 (105; 130)	0.00013
HR	70 (62; 80)	71 (65; 78)	67 (60; 80)	70 (63; 82)	0.26
NYHA III–IV	46 (46)	28 (35)	46 (55)	47 (75) ^a	< 0.0001
Diabetes mellitus	33 (33)	18 (23)	27 (32)	20 (32)	0.43
Hypertension	61 (60)	22 (28) ^a	48 (57)	36 (57)	< 0.0001
Dyslipidaemia	48 (48)	24 (30)	44 (53)	36 (57)	0.0045
History of AF	19 (19)	15 (19)	32 (38)	41 (66) ^a	< 0.0001
AF during echocardiography	5 (5)	3 (4)	19 (25)	31 (57)	< 0.0001
CAD	30 (30)	23 (29)	51 (61) ^a	18 (29)	< 0.0001
COPD	17 (17)	13 (16)	16 (19)	7 (11)	0.63
Beta-blocker	89 (88)	71 (89)	76 (92)	54 (87)	0.83
ACE inhibitor/ARB	91 (90)	77 (96)	72 (88)	45 (73) ^a	0.00026
Aldosterone antagonist	28 (28)	26 (33)	28 (34)	12 (20) ^a	0.23
Diuretic	74 (73)	56 (70)	73 (88)	57 (92)	0.0009
ICD	87 (86)	74 (93)	71 (85)	30 (48) ^a	< 0.0001
Upgrading to CRT	9 (9)	14 (18)	18 (21)	36 (57)	< 0.0001
9-month percentage of BVP (%)	99 ± 3	94 ± 17	96 ± 10	98 ± 4	0.00081
Electrocardiogram data					
Baseline QRS duration (ms)	160 (150; 170)	160 (160; 180)	150 (138; 160) ^a	170 (160; 200)	< 0.0001
QRS morphology					< 0.0001
LBBB	86 (85)	64 (80)	53 (63) ^a	33 (52) ^a	
RBBB	2 (2)	0 (0)	5 (6)	0 (0)	
Non-specific IVCD	7 (7)	7 (9)	14 (17)	4 (6)	
RV pacing	6 (6)	9 (11)	7 (8)	25 (40) ^a	
Narrow QRS	0 (0)	0 (0)	5 (6)	1 (2)	
BVP QRS duration (ms)	125 (120; 140) ^a	140 (130; 160)	140 (125; 150)	140 (135; 160)	< 0.0001
Effective BVP	80 (79)	64 (81)	70 (89)	48 (84)	0.38
QRS narrowing	98 (97)	58 (74)	48 (61) ^a	53 (88)	< 0.0001
Biological data					
Creatinine (mg/L)	11 (9; 13)	10 (9; 13)	12 (10; 16) ^a	14 (12; 17) ^a	< 0.0001
BNP (pg/mL)	166 (74; 367) ^a	437 (214; 901)	642 (357; 1170)	1050 (524; 1976) ^a	< 0.0001
Lead position on chest X-ray					
Non-apical LV lead position	70 (76)	72 (95)	62 (82)	44 (80)	0.012
Lateral versus non-lateral LV lead position					0.015
Lateral (lateral)	37 (40)	29 (38)	40 (53)	31 (55)	
Posterior (lateral)	48 (52)	46 (60)	29 (38)	23 (43)	
Anterior (non-lateral)	0 (0)	1 (1)	2 (3)	0 (0)	
Anterolateral (non-lateral)	7 (8)	0 (0)	5 (7)	2 (4)	
RV lead position					0.19
Apical	5 (5)	8 (10)	8 (10)	12 (21)	
Free wall	16 (16)	8 (10)	11 (14)	6 (10)	
High septum	1 (1)	1 (1)	3 (4)	0 (0)	
Mid septum	72 (73)	60 (77)	55 (70)	37 (64)	
RVOT	4 (4)	1 (1)	2 (2)	3 (5)	
Echocardiographic data					
LVEDV (mL)	198 (169; 231) ^a	290 (246; 326) ^a	243 (199; 292)	207 (169; 238)	< 0.0001
LVESV (mL)	198 (169; 231)	290 (246; 326)	243 (199; 292)	207 (169; 238)	< 0.0001

Table 3 (Continued)

	Phenogroup 1 (n = 101)	Phenogroup 2 (n = 80)	Phenogroup 3 (n = 84)	Phenogroup 4 (n = 63)	Overall P
LVEF (%)	30 ± 4 ^a	24 ± 5 ^a	25 ± 6	27 ± 5	< 0.0001
GLS (%)	-9.5 (-11.5; -8.1) ^a	-6.3 (-7.6; -5)	-6.8 (-8.4; -5.2)	-7.4 (-8.9; -5.4)	< 0.0001
LV mass index (g/m ²)	139 (123; 158)	170 (147; 208)	147 (125; 174)	144 (124; 178)	< 0.0001
Cardiac output index (L/m ²)	2,5 (2,1; 2,9)	2,4 (2; 3)	2 (1,6; 2,4)	2 (1,6; 2,4)	< 0.0001
LA volume index (mL/m ²)	29 (22; 36) ^a	35 (28; 45)	40 (34; 49)	45 (41; 53) ^a	< 0.0001
E-wave deceleration time (ms)	208 (152; 289)	147 (122; 223)	139 (120; 179)	139 (118; 172)	< 0.0001
E-wave velocity (m/s)	0.6 (0.5; 0.8)	0.7 (0.5; 0.9)	0.9 (0.7; 1.1)	0.9 (0.8; 1.1)	< 0.0001
E/A ratio	0.6 (0.5; 0.8)	0.9 (0.6; 1.7)	1.6 (0.9; 2.3)	2.1 (1.4; 3.3)	< 0.0001
E/E' ratio	11 (9; 13)	12.5 (10; 15)	16 (11; 18)	17 (12; 21)	< 0.0001
Mitral ERO (mm ²)	0 (0; 0)	0 (0; 8)	3 (0; 10)	8 (0; 14)	< 0.0001
Number of LV scarred segments	0 ± 1	0 ± 1	3 ± 2 ^a	0 ± 2	< 0.0001
RV diameter (mm)	29 ± 6 ^a	30 ± 7 ^a	32 ± 7	35 ± 6	< 0.0001
RA volume index (mL/m ²)	32 (22; 42)	41 (30; 57)	57 (38; 81) ^a	72 (54; 96) ^a	< 0.0001
TR peak velocity (m/s)	2.6 ± 0.5	2.7 ± 0.5	3 ± 0.6	3 ± 0.5	< 0.0001
Estimated RA pressure (mmHg)	3 (3; 5)	3 (3; 5)	5 (3; 10)	15 (8; 15)	< 0.0001
TAPSE (mm)	22 (20; 25)	20 (18; 23)	17 (14; 20)	16 (13; 20)	< 0.0001
Grade 3 or 4 TR	2 (2)	2 (3)	9 (11)	21 (33) ^a	< 0.0001
Interventricular dyssynchrony: IVMD (ms)	50 (35; 66)	59 (44; 72)	24 (0; 44) ^a	52 (33; 66)	< 0.0001
Atrioventricular dyssynchrony: ratio of LV filling and RR interval (%)	39 ± 7	37 ± 9	42 ± 9	41 ± 10	0.003
Septal flash	62 (98)	63 (98)	27 (47) ^a	37 (88)	< 0.0001
Apical rocking	67 (88)	53 (86)	9 (14) ^a	27 (84)	< 0.0001
Longitudinal LBBB classical pattern	95 (99)	75 (97)	51 (62) ^a	55 (97)	< 0.0001
Radial LBBB classical pattern	40 (62)	39 (80)	10 (19) ^a	13 (54)	< 0.0001
Septal deformation pattern 1 or 2	83 (82)	65 (81)	9 (12) ^a	37 (57)	< 0.0001
Response to CRT					
Changes in LVESV (mL)	-65 (-87; -42)	-79 (-121; -45)	-22 (-67; 4)	-54 (-88; -18)	< 0.0001
Relative changes in LVESV (%)	-51 (-58; -36)	-40 (-54; -23)	-11 (-35; 3)	-41 (-58; -14)	< 0.0001
Response to CRT	82 (81)	62 (78)	33 (39)	37 (59)	< 0.0001
Super-response to CRT	57 (65)	22 (29)	9 (13)	19 (37)	< 0.0001

Quantitative data are expressed as mean ± standard deviation or median (25th; 75th percentile); qualitative data are expressed as absolute number (%). ACE: angiotensin-converting enzyme; AF: atrial fibrillation; ARB: angiotensin receptor blocker; BMI: body mass index; BNP: brain natriuretic peptide; BVP: biventricular pacing; CAD: coronary artery disease; COPD: chronic obstructive pulmonary disease; CRT: cardiac resynchronization therapy; ERO: effective regurgitant orifice; GLS: global longitudinal strain; HR: heart rate; ICD: implantable cardioverter defibrillator; IVCD: intraventricular conduction delay; IVMD: interventricular mechanical delay; LA: left atrial; LBBB: left bundle branch block; LV: left ventricular; LVEDV: left ventricular end-diastolic volume; LVEF: left ventricular ejection fraction; LVESV: left ventricular end-systolic volume; NYHA: New York Heart Association; RA: right atrial; RBBB: right bundle branch block; RV: right ventricular; RVOT: right ventricular outflow tract; SBP: systolic blood pressure; TAPSE: tricuspid annular plane systolic excursion; TR: tricuspid regurgitation.

^a Characteristic feature of the phenogroup.

indications for CRT according to current guidelines. The findings from the present study may provide important information to refine CRT indications in ‘individualized’ clinical practice.

The differences between the four phenogroups (as shown in Table 2) were striking. Phenomapping analyses identified two phenogroups of patients (phenogroups 1 and 2) with the highest CRT response rates and most

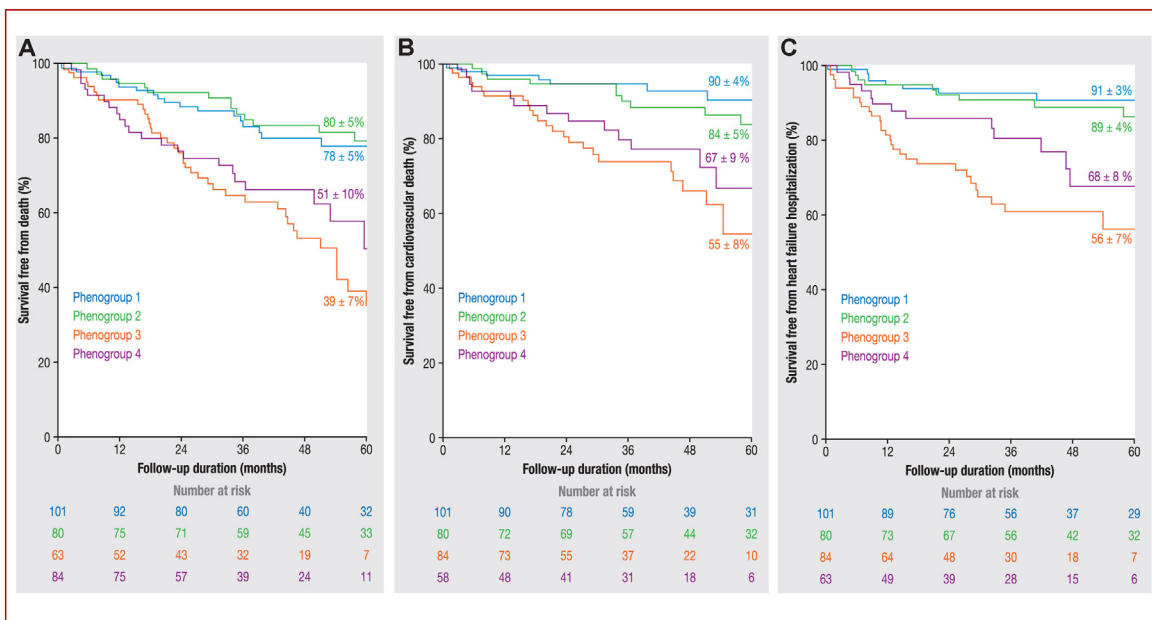


Figure 3. Survival free from (A) all-cause mortality; (B) cardiovascular mortality; and (C) heart failure hospitalization for each phenogroup of patients.

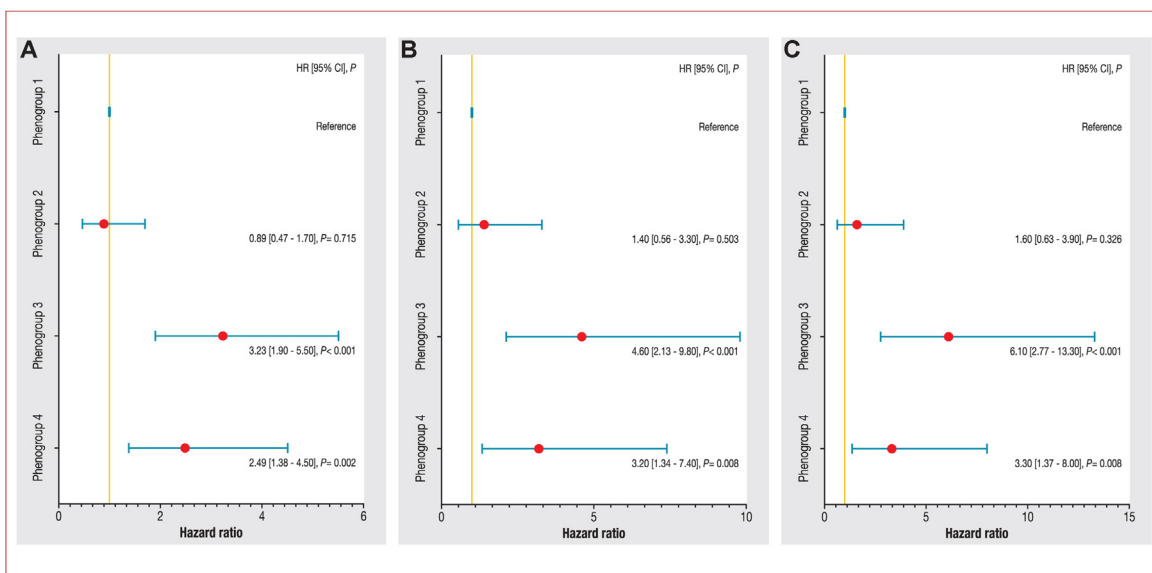


Figure 4. Hazard ratios for (A) all-cause mortality; (B), cardiovascular mortality; and (C) and heart failure hospitalization for each phenogroup of patients. CI: confidence interval; HR: hazard ratio.

improved outcome following CRT. Interestingly, although patients from phenogroups 1 and 2 had electrical and echocardiographic electromechanical dyssynchrony (with a very high frequency of septal flash and septal deformation pattern 1 or 2), patients from phenogroup 2 had a large LV and severely depressed LV function. However, those two phenogroups shared the same outcome and CRT response rate, with a higher proportion of CRT super-response in phenogroup 1. Hence, patients from phenogroup 1 may indeed correspond to patients with LBBB-induced cardiomyopathy (“dyssynchronopathy”), in which LV dysfunction can be successfully reverted by CRT [24].

Paradoxically, in patients from phenogroup 2, severe LV dilation and systolic dysfunction—both classical detrimental prognostic factors in HFref—did not offset the benefits of CRT, providing the presence of both electrical and echocardiographic electromechanical dyssynchrony, absence of severe HF symptoms and/or echocardiographic signs of HF decompensation.

The unsupervised machine learning approach allows the identification of two phenogroups of patients who have a lower probability of CRT response. Patients from phenogroup 3 had a poor outcome following CRT, with a low CRT response rate. Indeed, patients from phenogroup 3 display the

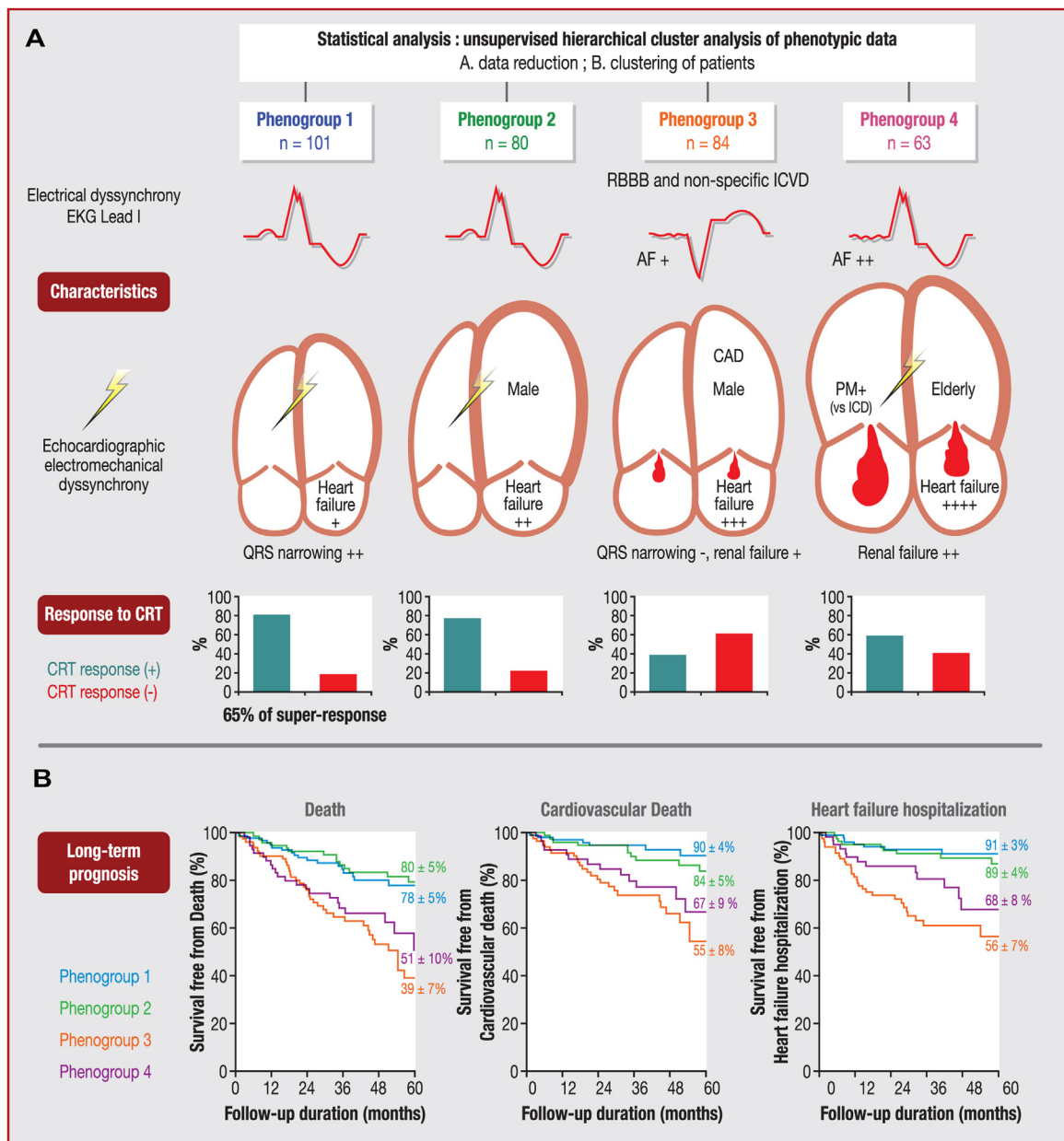


Figure 5. Central illustration. Clinical and prognostic implications of phenomapping in patients with heart failure receiving cardiac resynchronization therapy. AF: atrial fibrillation; CAD: coronary artery disease; CRT: cardiac resynchronization therapy; EKG: electrocardiogram; ICD: implantable cardioverter defibrillator; ICVD: intraventricular conduction delay; PM: pacemaker; RBBB: right bundle branch block.

classical features of non-response to CRT, including ischaemic cardiomyopathy and myocardial scarring, atrial fibrillation, decreased renal function, low prevalence of LBBB and narrower QRS duration. In addition, patients from phenogroup 3 had severely depressed LV function and enlarged LVs, but, in contrast to patients from phenogroup 2, they were characterized by absence of echocardiographic electromechanical dyssynchrony and lack of QRS narrowing following CRT—conditions that have a cumulative unfavourable impact on outcome in patients with HF receiving CRT [4]. Interestingly, in a recent study on animals and humans, Aalen et al. demonstrated that LV lateral wall dysfunction and scar abolished septal flash and markedly improved septal function in LBBB. Add ref 25 Consistently,

88% of patients from the phenogroup 3 had a septal pattern 3, characterized by a pseudonormalized septal pattern with no or minimal septal flash and preserved septal deformation. Therefore, the present phenomapping study demonstrates, as suggested by Aalen et al. [25], that the potential for improvement in these patients without an abnormal septal pattern is less than in those with abnormal septal motion. Whether these patients should not receive CRT cannot be ascertained from the present study, but should be investigated in future prospective studies, given their very poor outcome following CRT.

Interestingly, patients from phenogroup 4 also had a poor outcome. However, the CRT response rate was higher in these patients than in patients from phenogroup 3. These

patients were older, more frequently had co-morbidities and consequently received an ICD-CRT less frequently. Logically, they displayed characteristics of a restrictive cardiac physiology. A high proportion of patients from these phenogroups had RV pacing and electromechanical dyssynchrony. The finding that these patients share a similar poorer outcome in terms of mortality compared with patients from phenogroup 3, despite a relatively high CRT response rate, suggests that the clinical outcome of these patients may be primarily driven by co-morbidities, and highlights the importance of the global assessment of this particular phenogroup of patients, who are under-represented in randomized controlled therapeutic trials. However, the specific causes of non-cardiovascular mortality were not recorded in our database, thereby limiting the exploration of this hypothesis. Importantly, these patients were less frequently rehospitalized for HF during follow-up than patients from phenogroup 3, which may be an effective approach to decrease the socioeconomic burden of these frail patients.

The application of machine learning techniques has been seldom used in patients receiving CRT [26,27]. Cikes et al. used a similar approach to that in our study, using a non-supervised machine learning approach, and identified four phenogroups of patients with different degrees of CRT prognosis and response [26]. The present study builds on this report, as the machine learning approach was applied here on data from a real-life clinical setting, in contrast to the study by Cikes et al., which involved patients from the MADIT-CRT study, a randomized controlled study, with 36% of patients not receiving CRT, but an ICD alone. In addition, patients with RV pacing were excluded from the study by Cikes et al, whereas this condition was strongly associated with phenogroup 4 in the present report. In addition, Feeny et al. observed that nine variables (QRS morphology, QRS duration, New York Heart Association classification, LVEF, LV end-diastolic diameter, sex, ischaemic cardiomyopathy, atrial fibrillation and epicardial left ventricular lead) seemed to be sufficient to predict outcome after CRT [27]. However, Feeny et al. used a supervised approach to build a score with external validation, whereas our study was unsupervised and descriptive. Nevertheless, these studies have demonstrated the robustness of the machine learning approach to identify homogeneous groups of patients with a similar outcome in the field of CRT. Given the results of the present study, one may provocatively speculate that the clinical benefit of CRT is uncertain in patients from phenogroup 3. Hence, randomized control studies may be performed in patients sharing the characteristics of this phenogroup, whereas the performance of such a study would be probably not meaningful in patients from phenogroup 1 and 2, given their excellent outcome and CRT response rate.

Study limitations

The present study is a post hoc analysis of a prospective study. However, all data were prospectively collected, and the machine learning approach was unsupervised and performed by an investigator blinded to outcome data. The sample size of this monocentric study population was relatively small. However, the cohort constituted consecutive patients implanted in a real-life clinical practice, in contrast to post hoc analysis of randomized controlled therapeutic

trials [26]. Cardiac magnetic resonance imaging was not systematically performed in the present study; hence, the global and lateral wall scar burden cannot be evaluated.

Conclusions

Among patients with HF_rEF and an indication for CRT according to current guidelines, phenomapping identifies subgroups of patients with differential clinical, biological and echocardiographic features strongly linked to outcome and response to CRT. This approach may help to identify patients who are more likely to benefit from CRT in “individualized” clinical practice.

Sources of funding

No extramural funding was used to support this work.

Appendix A. Supplementary data

Supplementary data associated with this article can be found, in the online version, at <https://doi.org/10.1016/j.acvd.2020.07.004>.

Disclosure of interest

Y.G.: consulting fees from the companies St. Jude Medical and Medtronic.

The other authors declare that they have no competing interest.

References

- [1] McMurray JJ, Adamopoulos S, Anker SD, et al. ESC Guidelines for the diagnosis and treatment of acute and chronic heart failure 2012: the Task Force for the Diagnosis and Treatment of Acute and Chronic Heart Failure 2012 of the European Society of Cardiology. Developed in collaboration with the Heart Failure Association (HFA) of the ESC. *Eur Heart J* 2012;33:1787–847.
- [2] Holzmeister J, Leclercq C. Implantable cardioverter defibrillators and cardiac resynchronization therapy. *Lancet* 2011;378:722–30.
- [3] Altes A, Appert L, Delelis F, et al. Impact of increased right atrial size on long-term mortality in patients with heart failure receiving cardiac resynchronization therapy. *Am J Cardiol* 2019;123:936–41.
- [4] Appert L, Menet A, Altes A, et al. Clinical significance of electromechanical dyssynchrony and QRS narrowing in patients with heart failure receiving cardiac resynchronization therapy. *Can J Cardiol* 2019;35:27–34.
- [5] Bernard A, Menet A, Marechaux S, et al. Predicting clinical and echocardiographic response after cardiac resynchronization therapy with a score combining clinical, electrocardiographic, and echocardiographic parameters. *The Am J Cardiol* 2017;119:1797–802.
- [6] Brignole M, Auricchio A, Baron-Esquivias G, et al. 2013 ESC Guidelines on cardiac pacing and cardiac resynchronization therapy: the Task Force on cardiac pacing and resynchronization therapy of the European Society of Cardiology (ESC).

- Developed in collaboration with the European Heart Rhythm Association (EHRA). *Eur Heart J* 2013;34:2281–329.
- [7] Cleland JG, Abraham WT, Linde C, et al. An individual patient meta-analysis of five randomized trials assessing the effects of cardiac resynchronization therapy on morbidity and mortality in patients with symptomatic heart failure. *Eur Heart J* 2013;34:3547–56.
- [8] Leong DP, Hoke U, Delgado V, et al. Right ventricular function and survival following cardiac resynchronisation therapy. *Heart* 2013;99:722–8.
- [9] Marechaux S, Menet A, Guyomar Y, et al. Role of echocardiography before cardiac resynchronization therapy: new advances and current developments. *Echocardiography* 2016;33:1745–52.
- [10] Menet A, Bardet-Bouchery H, Guyomar Y, et al. Prognostic importance of postoperative QRS widening in patients with heart failure receiving cardiac resynchronization therapy. *Heart Rhythm* 2016;13:1636–43.
- [11] Menet A, Bernard A, Tribouilloy C, et al. Clinical significance of septal deformation patterns in heart failure patients receiving cardiac resynchronization therapy. *Eur Heart J Cardiovasc Imaging* 2017;18:1388–97.
- [12] Rossi L, Malagoli A, Piepoli M, et al. Indexed maximal left atrial volume predicts response to cardiac resynchronization therapy. *Int J Cardiol* 2013;168:3629–33.
- [13] Stankovic I, Prinz C, Ciarka A, et al. Relationship of visually assessed apical rocking and septal flash to response and long-term survival following cardiac resynchronization therapy (PREDICT-CRT). *Eur Heart J Cardiovasc Imaging* 2015;17:262–9.
- [14] Surawicz B, Childers R, Deal BJ, et al. AHA/ACCF/HRS recommendations for the standardization and interpretation of the electrocardiogram: part III: intraventricular conduction disturbances: a scientific statement from the American Heart Association Electrocardiography and Arrhythmias Committee, Council on Clinical Cardiology; the American College of Cardiology Foundation; and the Heart Rhythm Society. Endorsed by the International Society for Computerized Electrocardiology. *J Am Coll Cardiol* 2009;53:976–81.
- [15] Thebault C, Donal E, Meunier C, et al. Sites of left and right ventricular lead implantation and response to cardiac resynchronization therapy observations from the REVERSE trial. *Eur Heart J* 2012;33:2662–71.
- [16] Lang RM, Badano LP, Mor-Avi V, et al. Recommendations for cardiac chamber quantification by echocardiography in adults: an update from the American Society of Echocardiography and the European Association of Cardiovascular Imaging. *J Am Soc Echocardiogr* 2015;28, 1-39 e14.
- [17] Menet A, Greffe L, Ennezat PV, et al. Is mechanical dyssynchrony a therapeutic target in heart failure with preserved ejection fraction? *Am Heart J* 2014;168, 909-16 e1.
- [18] Lumens J, Tayal B, Walmsley J, et al. Differentiating electromechanical from non-electrical substrates of mechanical discoordination to identify responders to cardiac resynchronization therapy. *Circ Cardiovasc Imaging* 2015;8:e003744.
- [19] Risum N, Tayal B, Hansen TF, et al. Identification of typical left bundle branch block contraction by strain echocardiography is additive to electrocardiography in prediction of long-term outcome after cardiac resynchronization therapy. *J Am Coll Cardiol* 2015;66:631–41.
- [20] Leenders GE, Lumens J, Cramer MJ, et al. Septal deformation patterns delineate mechanical dyssynchrony and regional differences in contractility: analysis of patient data using a computer model. *Circ Heart Fail* 2012;5:87–96.
- [21] Marechaux S, Guiot A, Castel AL, et al. Relationship between two-dimensional speckle-tracking septal strain and response to cardiac resynchronization therapy in patients with left ventricular dysfunction and left bundle branch block: a prospective pilot study. *J Am Soc Echocardiogr* 2014;27:501–11.
- [22] Chavent M, Kuentz Simonet V, Liquet B, Saracco J, An R. Package for the clustering of variables. *J Stat Softw* 2012;1–16.
- [23] Rand WM. Objective criteria for the evaluation of clustering methods. *J Am Stat Assoc* 1971;66:846–50.
- [24] Vaillant C, Martins RP, Donal E, et al. Resolution of left bundle branch block-induced cardiomyopathy by cardiac resynchronization therapy. *J Am Coll Cardiol* 2013;61:1089–95.
- [25] Aalen JM, Remme EW, Larsen CK, et al. Mechanism of abnormal septal motion in left bundle branch block: role of left ventricular wall interactions and myocardial scar. *JACC Cardiovasc Imaging* 2019;12:2402–13.
- [26] Cikes M, Sanchez-Martinez S, Claggett B, et al. Machine learning-based phenogrouping in heart failure to identify responders to cardiac resynchronization therapy. *Eur J Heart Fail* 2019;21:74–85.
- [27] Feeny AK, Rickard J, Patel D, et al. Machine learning prediction of response to cardiac resynchronization therapy. *Circ Arrhythm Electrophysiol* 2019;12:e007316.